

See discussions, stats, and author profiles for this publication at: <https://www.researchgate.net/publication/265735190>

Programmable biofilm-based materials from engineered curli nanofibres

Article *in* Nature Communications · September 2014

DOI: 10.1038/ncomms5945 · Source: PubMed

CITATIONS

27

READS

719

4 authors, including:



Peter Q Nguyen

Harvard University

20 PUBLICATIONS 112 CITATIONS

[SEE PROFILE](#)



Richie Tay

Harvard University

3 PUBLICATIONS 108 CITATIONS

[SEE PROFILE](#)



Neel Joshi

Harvard University

24 PUBLICATIONS 720 CITATIONS

[SEE PROFILE](#)

All content following this page was uploaded by [Neel Joshi](#) on 25 November 2014.

The user has requested enhancement of the downloaded file. All in-text references [underlined in blue](#) are added to the original document and are linked to publications on ResearchGate, letting you access and read them immediately.

1
2
3
4
5
6
7
8 **Programmable Biofilm-Based Materials from Engineered Curli Nanofibers**

9
10 Peter Q. Nguyen^{1,2}, Zsofia Botyanszki^{2,3}, Pei Kun R. Tay^{1,2} and Neel S. Joshi^{1,2*}

11
12
13 School of Engineering and Applied Sciences¹,
14 Wyss Institute for Biologically Inspired Engineering²,
15 Department of Chemistry and Chemical Biology³,
16 Harvard University, Cambridge, MA 02138, USA.

17
18
19
20
21
22
23
24
25
26
27
28
29
30
31
32 *Corresponding Author:

33 Dr. Neel S. Joshi
34 School of Engineering and Applied Sciences /
35 Wyss Institute for Biologically Inspired Engineering
36 Harvard University
37 Cambridge, MA 02138, USA.

38 Tel: (617) 432-7732
39 E-Mail: njoshi@seas.harvard.edu

1 **Abstract**

2 The significant role of biofilms in pathogenicity has spurred research into preventing their
3 formation and promoting their disruption, resulting in overlooked opportunities to develop
4 biofilms as a synthetic biological platform for self-assembling functional materials. Here we
5 present “Biofilm-Integrated Nanofiber Display” (BIND) as a strategy for the molecular
6 programming of the bacterial extracellular matrix material by genetically appending peptide
7 domains to the amyloid protein CsgA, the dominant proteinaceous component in *E. coli* biofilms.
8 These engineered CsgA fusion proteins are successfully secreted and extracellularly self-
9 assemble into amyloid nanofiber networks that retain the functions of the displayed peptide
10 domains. We show the use of BIND to confer diverse artificial functions to the biofilm matrix,
11 such as nanoparticle biotemplating, substrate adhesion, covalent immobilization of proteins, or a
12 combination thereof. BIND is a versatile nanobiotechnological platform for developing robust
13 materials with programmable functions, demonstrating the potential of utilizing biofilms as
14 large-scale designable biomaterials.

15

1 **Introduction**

2 Advances in our understanding of bacterial systems in the past century have expanded the
3 role of the microbe from being regarded solely as a health threat to being exploited as a
4 genetically programmable factory for the production of biomolecules and chemicals. We view
5 bacterial biofilms as embarking on a similar trajectory vis-à-vis functional advanced materials.
6 The majority of bacteria in the natural world exist as biofilms: organized communities of cells
7 ensconced in a network of extracellular matrix (ECM) composed of polysaccharides, proteins,
8 nucleic acids, and other biomolecular components¹. This self-generated ECM protects bacteria
9 from environmental rigors and mediates substrate adhesion, thus promoting microbial
10 persistence and pathogenicity. Hence, the majority of biofilm research has focused on their
11 eradication due to the negative roles biofilms play in clinical infection².

12 We envision instead the domestication of biofilms as a platform for programmable and
13 modular self-assembling extracellular nanomaterials, with the bacterium serving as a living
14 foundry for the synthesis of raw building blocks, their assembly into higher order structures upon
15 secretion, and the maintenance of the material as a whole over time. While there has been some
16 investigation into the use of biofilms for beneficial purposes such as energy generation³,
17 wastewater treatment⁴ and biotransformations^{5,6}, these studies have primarily focused on altering
18 the population of the biofilm microbial consortia rather than the ECM material itself. Another
19 example is recent exciting work from the Wood group, in which they describe the design of
20 synthetic genetic circuits that modulate the population balance in a dual-species biofilm to
21 control biofilm formation and dispersal based on quorum-sensing⁷.

22 Our approach to engineering the biofilm ECM material for practical applications focuses
23 on the curli system – the primary proteinaceous structural component of *E. coli* biofilms. Curli

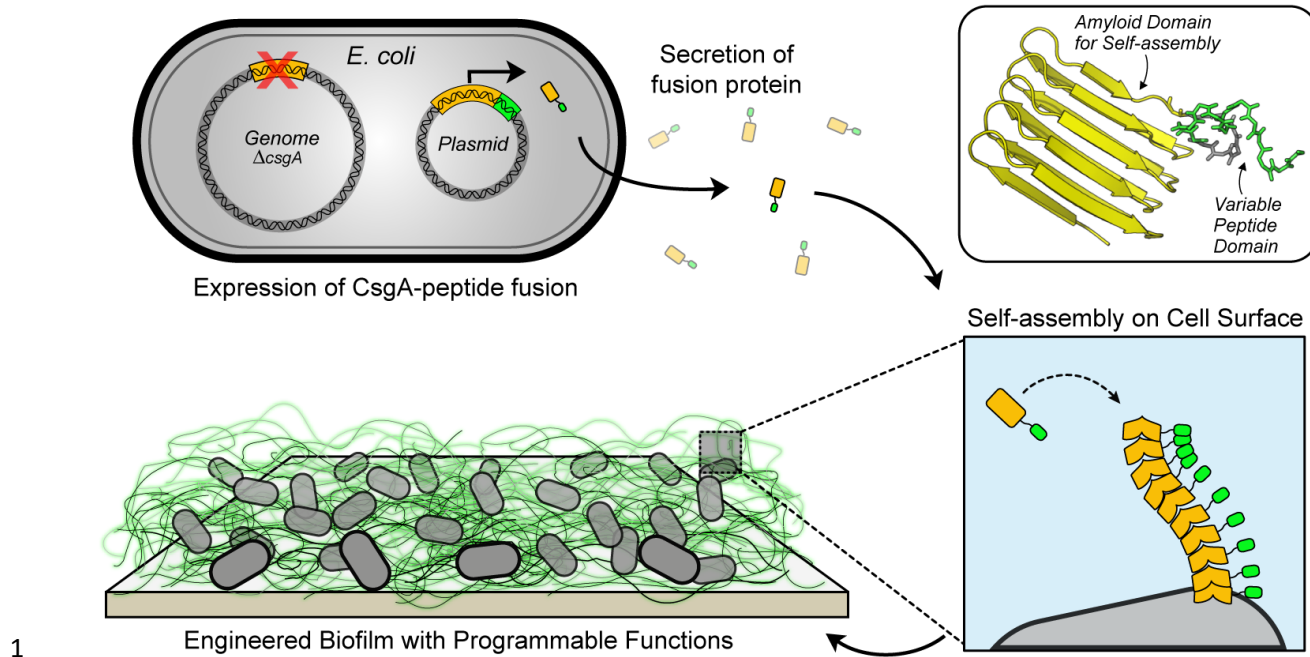
1 are highly robust functional amyloid nanofibers with a diameter of ~4-7 nm that exist as
2 extended tangled networks encapsulating the cells. Curli are formed from the extracellular self-
3 assembly of CsgA, a small secreted 13-kDa protein. A homologous outer-membrane protein,
4 CsgB, nucleates CsgA assembly and also anchors the nanofibers to the bacterial surface.
5 Detached curli fibers can also exist as non-cell associated structural components of the ECM.
6 The curli genes exist as two divergently transcribed operons (*csgBAC* and *csgDEFG*)⁸, whose
7 seven products mediate the structure (CsgA), nucleation (CsgB), processing (CsgE, F), secretion
8 (CsgC, G), and direct transcriptional regulation (CsgD) of curli nanofibers.

9 The curli system exhibits numerous features that make it an ideal platform for the type of
10 materials engineering by way of synthetic biology that we envision. First, since the curli
11 nanofiber is composed primarily from the self-assembly of one small protein, it presents a
12 tractable entry point towards creating a large diversity of biofilm extracellular matrices with
13 conventional genetic engineering methods. In contrast, it would be more difficult to engineer the
14 exopolysaccharide component of biofilms, as polysaccharide synthesis is often tied to multi-step
15 pathways with a limited tolerance for chemically diverse monomers compared to the protein
16 synthetic machinery. Second, the functional amyloid fibers formed by CsgA are extremely
17 robust, being able to withstand boiling in detergents⁹ and extended incubation in solvents,
18 increasing their potential utility in harsh environments. Similar amyloid nanofibers have been
19 shown to have a strength comparable to steel and a mechanical stiffness comparable to silk¹⁰,
20 suggesting that biofilms with high amyloid content would be able to withstand mechanically
21 demanding environments. Third, functional amyloid fibrils are abundant in many naturally
22 occurring bacterial biofilms and can constitute up to 10-40% of the total biovolume of a
23 biofilm¹¹, indicating that curli can be artificially engineered to comprise a significant portion of

1 the biofilm. In addition, although analogous extracellular functional amyloids are produced by
2 many bacteria, the curli system is currently the best studied and is native to the canonical model
3 bacterium *E. coli*, making it an attractive starting platform for the development of engineered
4 materials. Finally, recent findings have shown that the curli system can be used to efficiently
5 export natively unfolded polypeptides and was capable of producing a functional camelid
6 antibody fragment, suggesting that the curli system can be used in a broad and modular way for
7 the display of various functional peptides throughout the *E. coli* biofilm ECM^{12,13}.

8 Here we show that the BIND system enables precise genetic programming of the *E. coli*
9 biofilm extracellular matrix material by fusing functional peptide domains onto the CsgA
10 protein. We demonstrate that the chimeric CsgA variants are secreted by the native cellular
11 export machinery and assemble into networks of curli fibers resembling the wild-type system.
12 We also show that this technique is compatible with a wide range of peptide domains of various
13 lengths and secondary structures. Lastly, we demonstrate that the peptide domains maintain their
14 function after secretion and assembly and confer artificial functions to the biofilm as a whole.
15 Very recently, Chen et al. have demonstrated a parallel curli-based system similar to our BIND
16 concept, and show controlled multiscale patterning of single amyloid fibers and the use of
17 engineered curli for the organization of gold nanoparticles and quantum dots for nanoelectronics
18 applications¹⁴. Herein, we expand on the functions that can be engineered into curli nanofibers
19 by demonstrating three broad functions that we artificially introduce into the *E. coli* biofilm
20 ECM: inorganic nanoparticle templating, specific abiotic substrate adhesion, and the site-specific
21 covalent immobilization of an arbitrary functionalized recombinant protein.

22



1 **Figure 1.**

2
3 **Results**
4

5 **Determination of an optimal peptide fusion site for CsgA.** The BIND strategy consists of
6 reprogramming the self-assembling amyloid component of *E. coli* biofilms using genetic fusions
7 of CsgA to functional peptides (Fig. 1). In order to determine suitable fusion points to append
8 peptides to CsgA, we generated a library (Fig. 2a) consisting of N- and C-terminal fusions to a
9 test peptide domain designated MBD (for Metal Binding Domain). The MBD peptide has been
10 shown to bind strongly to stainless steel surfaces and is derived from a segment of the
11 *Pseudomonas aeruginosa* type IV pilus¹⁵. CsgA-terminal fusions were chosen to allow for the
12 integration of both linear and circularly constrained peptides. Three variants were prepared for
13 each terminus with varying glycine-serine flexible linker lengths. We used the standard amyloid-
14 staining colorimetric dye, Congo Red¹⁶ (CR), to determine the extent of curli production for the
15 various mutants. The *csgA* variants were expressed in the model *E. coli csgA* deletion strain
16 LSR10 (MC4100::ΔcsgA) that retains the remaining curli processing machinery under native

1 regulation⁸. This strain has previously been used in numerous studies on the curli system as it has
2 been shown to not produce flagella, cellulose, or LPS O-polysaccharides, making it ideal for
3 curli complementation studies¹⁷⁻¹⁹. Thus, LSR10 was chosen as a model strain for developing
4 BIND in part because any colorimetric signal obtained from CR staining could be attributed to
5 the presence of heterologously produced curli fibers, as opposed to cellulose or other biofilm
6 components that may have the capability to bind CR non-specifically²⁰. Likewise, any
7 extracellular fibers observed by transmission electron microscopy (TEM) and scanning electron
8 microscopy (SEM) ultrastructural characterization can be attributed solely to the self-assembly
9 of heterologously engineered CsgA fusion mutants.

10 The CR staining assay of the MBD insertion library indicated only the C3 fusion site with
11 the longest C-terminal linker between CsgA and MBD was able to form an appreciable amount
12 of amyloid fibers (Fig. 2b), albeit at a lower amount than the wild-type CsgA. It is possible that
13 the N-terminal fusions had impaired secretion as a result of their proximity to the CsgG-specific
14 export recognition sequence. Ultrastructural characterization by SEM (Fig. 2n) and TEM
15 (Supplementary Figure 1k and Supplementary Figure 2j) of the C3 mutant curli nanofibers
16 confirmed that they exhibited morphology similar to that of the wild-type CsgA fibers.

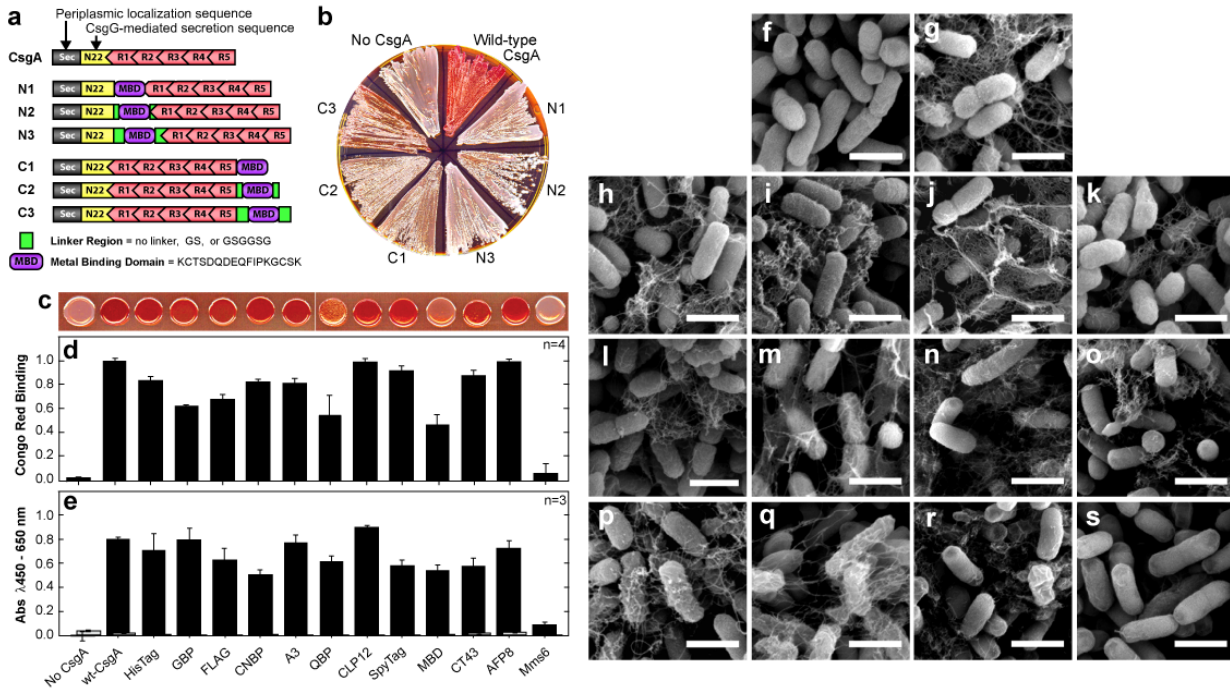


Figure 2.

CsgA peptide fusions retain amyloid self assembly function. Having identified the C3 fusion site as suitable for the display of peptides on the CsgA scaffold, we next created a library of 12 various peptide domain fusions to test the effect of peptide length and structure on secretion and assembly. The library members, detailed in Table 1, range in length from 7 to 59 amino acids and encode a wide variety of functions such as binding to various inorganic substrates (GBP, CNBP, QBP, MBD, and AFP8), nucleation of mineral and metallic nanostructures (A3, CLP12, CT43, and Mms6), and a highly specific catalytic interaction with a protein (SpyTag)^{15,21-31}. Each peptide domain was cloned as C-terminal fusions to CsgA with an intervening six-amino acid flexible linker (Table 1) and these plasmids were expressed in LSR10 cells to produce 12 different BIND biofilms.

14

1 Relative differences in curli production between library members were monitored by measuring
2 the staining intensity of transformants spotted on CR plates (Fig. 2c,d). CR binding is highly
3 indicative of amyloids, providing a qualitative assessment of CR-binding extracellular material.
4 These CR assays indicate that small peptide fusions may be tolerated by the curli export
5 machinery and could successfully assemble into extracellular amyloid networks as evidenced by
6 greater CR staining of all peptide fusions compared to the empty plasmid control. The only
7 mutant for which there was no positive CR staining was the 59-amino acid Mms6 protein
8 domain, confirming previous findings that polypeptides with long sequences or inherent structure
9 may not be exported efficiently through the CsgG outer membrane transporter, which has a pore
10 size of 2 nm³². As CR is also known to bind to other molecules in addition to amyloids, a more
11 specific assessment of the amyloid-nature of proteins is provided from birefringence of the CR-
12 stained material observed under polarized light³³⁻³⁵. Cell masses of the BIND colonies from
13 YESCA-CR plates were analyzed by polarization microscopy (Supplementary Figure 3). Most of
14 the BIND variants exhibited birefringence characteristic of amyloids, although the intensity of
15 the birefringence varied. The no curli control and Mms6-BIND samples showed no
16 birefringence, as expected. Surprisingly, the CLP12- and QBP-BIND samples showed very low
17 levels of birefringence, although they have high levels of CR binding. We posit that this is due to
18 the amyloid fibers being highly dispersed or the presence of these peptides altering the binding
19 mode of the CR such that birefringence is suppressed. To validate that the CR staining is due to
20 the presence of extracellular materials containing CsgA, such as curli fibers, we performed
21 whole-cell filtration ELISAs using anti-CsgA antibodies (Figure 2e). Only extracellular material
22 composed of CsgA and retained by the 0.22 µm filter would generate a CsgA-positive signal.
23 The whole-cell ELISA data correlates with the CR staining results, confirming that CsgA-

1 containing proteins are present extracellularly and are present as high molecular-weight
2 assemblies. The ELISA data does not discriminate intact fusion proteins from possible
3 breakdown products, however. To investigate the possibility that these extracellular amyloids are
4 due to the secretion and assembly of partially proteolyzed CsgA fusion proteins and not the
5 desired full-length CsgA fusion proteins, we isolated the extracellular fractions of induced BIND
6 colonies and subjected this fraction to SDS solubilization. The SDS-insoluble fraction was
7 collected by ultracentrifugation and dissolved in hexafluoroisopropanol (HFIP) to disassemble
8 the curli fibers into their monomeric components. MALDI-TOF/TOF analysis of the resulting
9 dissolved samples confirms the presence of mass peaks that correlate with the predicted mature
10 CsgA fusion proteins in all of the samples except for the no curli control and the Mms6-BIND
11 sample (Supplementary Figure 4). Although this does not rule out potential proteolysis events, it
12 does demonstrate that the extracellular fraction contains, to some degree, intact CsgA fusion
13 proteins that are in an SDS-insoluble state, suggesting that the desired proteins are assembled
14 into amyloid structures. It is possible amorphous extracellular aggregates could contribute to the
15 CR-binding, whole-cell ELISA, and MALDI results. To further confirm the presence of curli
16 nanofibers and rule out unstructured extracellular aggregates in the BIND biofilms, we
17 extensively analyzed the ultrastructure of the curli biofilms using SEM (Fig. 2f-s) and TEM
18 (Supplementary Figure 1). For the CR-positive transformants, fine nanofibers associated with the
19 cells were observed which are similar in morphology to wild-type CsgA. High magnification
20 TEM analysis of the BIND nanofibers revealed that they have a diameter of 4-7 nm, consistent
21 with that previously reported for curli nanofibers³⁶ (Supplementary Figure 2). The BIND
22 nanofibers displayed a characteristic tangled morphology and were observed to be closely
23 associated with the cell surface or sometimes existing as free-floating masses. No extracellular

1 fibers were observed for either the empty plasmid control or the Mms6-BIND biofilm (Fig. 2f,s
2 and Supplementary Figure 1a,n), corroborating the lack of CR staining and whole-cell ELISA
3 signals for these samples. We additionally performed immunogold labeling of the BIND biofilms
4 producing the CsgA-FLAG fusion protein, using an anti-FLAG antibody. The immunogold TEM
5 images show localization of the gold nanoparticles to the curli fiber tangles, confirming both the
6 presence and accessibility of the FLAG peptide domain (Supplementary Figure 5). In sum, the
7 CR staining and CR birefringence experiments demonstrate the presence of extracellular
8 amyloid, the whole-cell filtration ELISA data indicate that the CsgA fusions are present as
9 extracellular assemblies, the MALDI analysis confirms the presence of SDS-insoluble
10 extracellular material correlating in mass to the expected fusion proteins, and electron
11 microscopy imaging of the BIND biofilms provides ultrastructural verification of the
12 nanofibrillar morphology of the BIND ECM. Thus, peptides of arbitrary sequence and function
13 can be efficiently displayed as C-terminal fusions to CsgA for extracellular self-assembly into
14 functionalized curli nanofibers.

15 The true value of the BIND system is in its ability to perform as an expansive
16 interfacial biomaterial whose function can be genetically programmed in a modular fashion. As a
17 demonstration of some of these capabilities, we selected three peptides from Table 1 (FLAG, A3,
18 MBD, and SpyTag) with diverse functions and tested their ability to introduce these new
19 functions into curli-producing biofilms. Specifically, we investigated the ability to program
20 biotemplating of inorganic nanoparticles (A3), enhanced adhesion to abiotic surfaces (MBD),
21 and covalent immobilization of full-length proteins into the BIND biofilms (SpyTag). We also
22 examined the generation of multifunctional BIND biofilms (FLAG and SpyTag). For these
23 functional studies we chose a different cell strain as a chassis for robust curli production, a

1 previously developed *csgA* deletion mutant of the *E.coli* K-12 strain PHL628³⁷. Although they
2 also produce cellulose, which made them unsuitable for the initial characterization of the BIND
3 platform, the PHL628 (MG1655 *malA-Kan ompR234*) cells are superior to the LSR10 strain for
4 curli production due to a single point mutation in the OmpR protein which enhances expression
5 of the entire curli operon by ~3.5x, resulting in substantial amounts of curli production³⁸. This
6 phenotype is ideal for generating expansive amyloid-rich ECM for functional analysis; plasmid-
7 based overexpression of heterologous BIND variants in a $\Delta csgA$ PHL628 knockout mutant
8 (hereafter referred to just as PHL628) is likely to prevent accumulation of the fusion proteins
9 intracellularly by providing a high basal production of the proteins required for efficient
10 processing and secretion of the CsgA fusions. Expression of the entire BIND peptide library in
11 PHL628 cells resulted in similar relative curli production patterns as determined by CR binding
12 in comparison to the LSR10 strain (Supplementary Figure 6). We also performed whole-cell
13 filtration ELISAs on the FLAG-, A3-, SpyTag-, and MBD-BIND biofilms to show that the CsgA
14 protein is exported and assembles into a high molecular-weight extracellular material
15 (Supplementary Figure 7a,c,e,g). Furthermore, MALDI-TOF/TOF analysis of the SDS-insoluble
16 purified extracellular material shows mass peaks that correspond to that of the expected fusion
17 proteins, suggesting that they are present and unproteolyzed as amyloid fibrils in the ECM
18 (Supplementary Figure 7b,d,f,h).

19 **Silver nanoparticle templating onto A3 BIND nanofibers.** Engineered peptides functionalized
20 onto the ECM can also be used to promote materials templating, which we demonstrate using
21 BIND composed of a CsgA-A3 fusion produced in PHL628 cells. The A3 peptide was
22 previously developed by phage display to bind silver and has been shown to control the
23 templating of silver nanoparticles²⁵. The wild-type CsgA biofilm did not appreciably template

silver nanoparticles (Fig. 3a). In contrast, the A3-BIND biofilms show an enhanced ability to bind to growing silver nanoparticles from a solution of AgNO₃, as shown by representative TEM images of incubated A3-BIND showing the assembly of nanoparticles throughout the nanofibers. (Fig. 3b-c). These results are reproducible (Supplementary Figure 8) and demonstrate the utility of programmable biofilm matrices for the templating and organization of nanoparticles to form one-dimensional nanowires. The resulting nanoparticle-decorated nanofibers show a striking resemblance to naturally occurring metal-reducing extracellular fibers from *Geobacter sulfurreducens*, which have been shown to be electrically conductive³⁹, suggesting that BIND-based biotemplating may be a viable strategy for the large-scale *de novo* production of conductive nanowires.

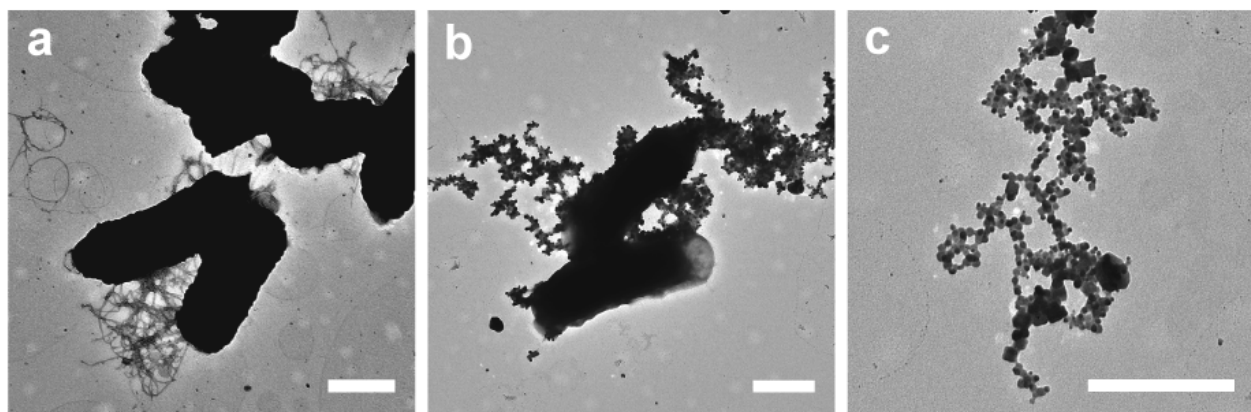


Figure 3.
Programmed BIND adhesion to 304L stainless steel. In order to make BIND an efficient platform for developing interfacial materials, it will be critical to tune the nanofiber adhesion to specific abiotic surfaces. As an example of this capability, we tested the adhesion of *E. coli* cells displaying MBD to 304L stainless steel, the most versatile and widely used steel alloy. PHL628 cells producing the CsgA-MBD mutant were spotted onto 304L coupons (Fig. 4a), allowed to adhere for 48 hours, and then vigorously washed by vortexing at a high setting in aqueous buffer to thoroughly remove non-specifically bound cells. The spotted areas were analyzed by SEM and

1 showed that BIND composed of the CsgA-
2 MBD fusion withstood the washing
3 procedure (Fig. 3b-d), while the no CsgA or
4 wild-type CsgA control cells were washed
5 off the surface (Supplementary Figure 9).
6 This result demonstrates that BIND
7 programming using MBD is sufficient to
8 impart adhesive function to biofilms that
9 can withstand very rigorous washing
10 conditions. The modularity of the BIND
11 platform lends itself to a plug-and-play
12 approach for the design of programmed
13 biofilm adhesion for applications in

14 bioremediation or chemical synthesis, where non-specific biofilm growth is viewed as a
15 disadvantage. This capability will be particularly useful in applications where patterned surfaces
16 are used to spatially control biofilm formation⁴⁰, or where it is desirable to localize biofilm
17 growth to specific materials and resist detachment forces, as is often the case in industrial
18 bioreactors^{41,42}.

19 **Covalent immobilization of proteins using BIND.** In addition to displaying short peptides, we
20 reasoned that the utility of the BIND system would be greatly expanded if it could be used to
21 display full proteins of arbitrary length and dimensions to program the biofilm with artificial
22 enzymatic, electron transport, or sensing capabilities. We therefore created a two-component
23 genetically encodable strategy (Fig. 5a) to covalently immobilize proteins onto the BIND

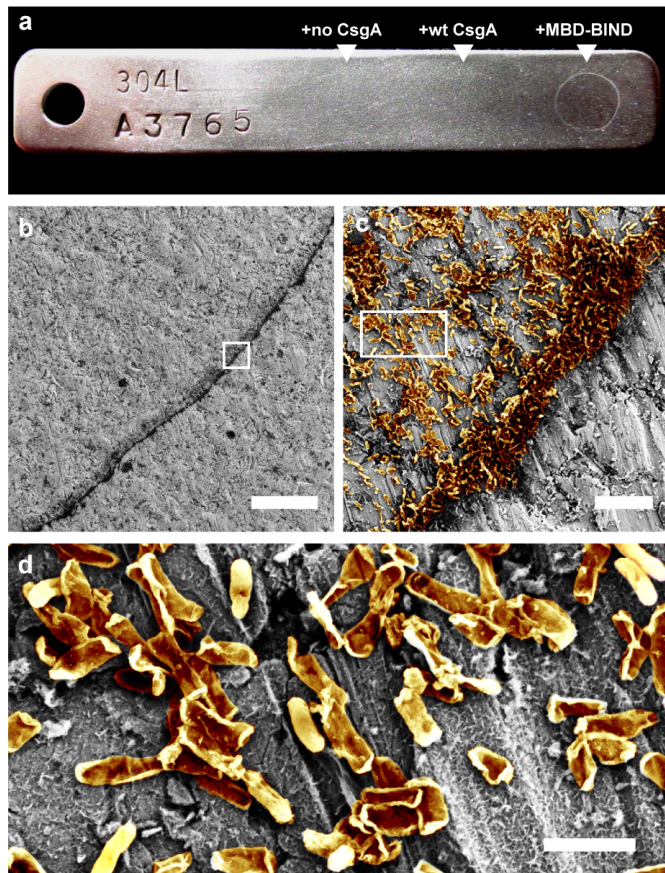
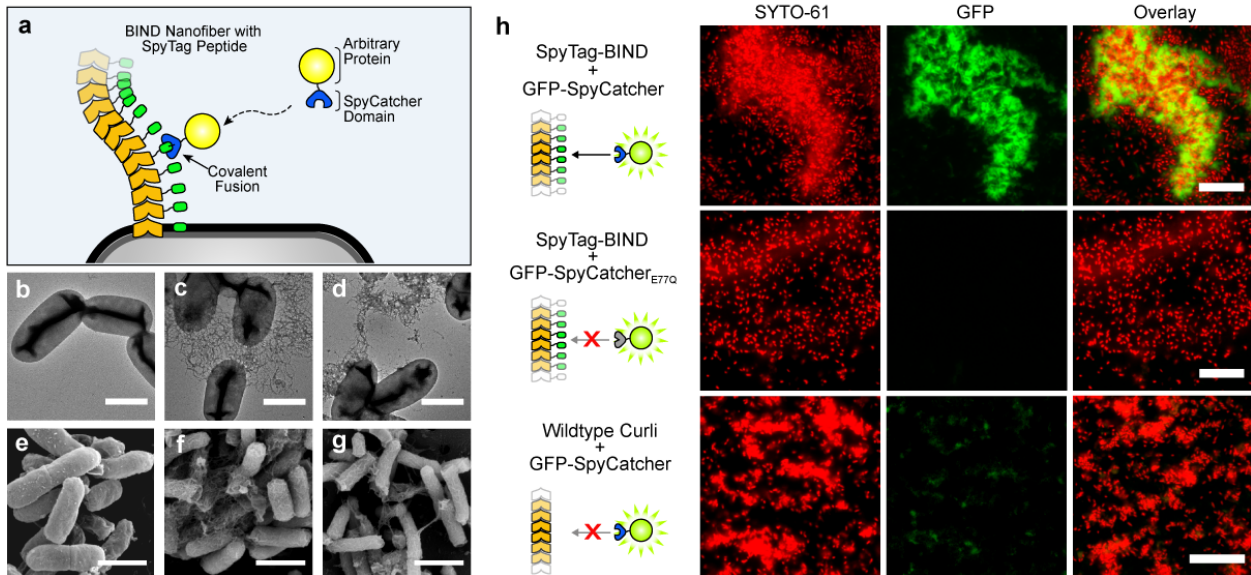


Figure 4.

1 network, using a previously developed split-adhesin system²⁸ in which a 13-amino acid peptide
2 (SpyTag) forms a highly specific and spontaneous isopeptide bond with a 15-kDa protein
3 (SpyCatcher). The first component of our protein immobilization approach is an engineered
4 SpyTag-functionalized BIND ECM and the second component is a SpyCatcher protein fused to
5 another protein of interest. As our arbitrary test protein for ECM-immobilization, we chose GFP.
6 SpyTag-BIND biofilms were grown on a glass substrate using PHL628 cells and formed
7 characteristic curli nanofiber networks when either wild-type CsgA or CsgA-SpyTag were
8 produced (Fig. 5b-g). We recombinantly produced GFP-SpyCatcher and a non-functional
9 mutant²⁸ (GFP-SpyCatcher_{E77Q}) and applied cell lysates containing these proteins to SpyTag-
10 BIND or wild-type CsgA biofilms. Analysis by epifluorescence microscopy revealed, as
11 expected, that only the combination of biofilms composed of CsgA-SpyTag incubated with GFP-
12 SpyCatcher resulted in covalent attachment (Fig. 5h). To further validate that the GFP-
13 SpyCatcher is localized to the extracellular material and not to the cells, we analyzed SpyTag-
14 BIND + GFP-SpyCatcher samples using confocal microscopy and aligned the high-resolution
15 fluorescence images with SEM micrographs of the same sample (Supplementary Figure 10a-c).
16 Regions that are fluorescent (Supplementary Figure 10d,e,g,h) clearly correlate to regions that
17 have a high density of ECM (Supplementary Figure 10e,f,h,i). These results confirm that the
18 SpyTag peptide can be fused to CsgA and maintain its functionality as a catalytic covalent
19 immobilization tag after extracellular assembly into curli nanofibers. Furthermore, the use of
20 unpurified cell lysate containing the GFP-SpyCatcher fusion protein demonstrates the robust
21 binding specificity between the SpyTag-functionalized curli network and the SpyCatcher fusion
22 protein, even in complex mixtures. This feature of BIND will be especially useful in the

1 development of biocatalysts and biosensors, for the development of a facile and efficient enzyme
2 immobilization process.



4 **Figure 5.**

5
6
7 **BIND can be used to engineer multifunctional biofilms.** Previous research has shown that
8 cross-seeding between even distantly related amyloid proteins can occur, resulting in composite
9 nanofibers⁴³. A key aspect of our BIND system is that by virtue of the random extracellular self-
10 assembly of CsgA monomers, the simultaneous secretion of different CsgA fusions will result in
11 a formation of a multifunctional biofilm surface. To demonstrate the generation of a biofilm
12 ECM containing multiple artificially-designed functions, we co-cultured PHL628 cells producing
13 CsgA-FLAG and CsgA-SpyTag fusion proteins to produce a bifunctional BIND biofilm that can
14 display the FLAG tag as well as immobilize GFP through the SpyTag-SpyCatcher system (Fig.
15 6). Only the co-cultured sample is able to co-localize the GFP-SpyCatcher and a fluorescently-
16 labeled anti-FLAG antibody, as visualized by confocal microscopy (Fig. 6, bottom row). This
17 capability of engineering multifunctional biofilms greatly increases the utility of our system for

- 1 complex applications which require any combination of adhesion, display, molecular templating,
- 2 or protein immobilization.

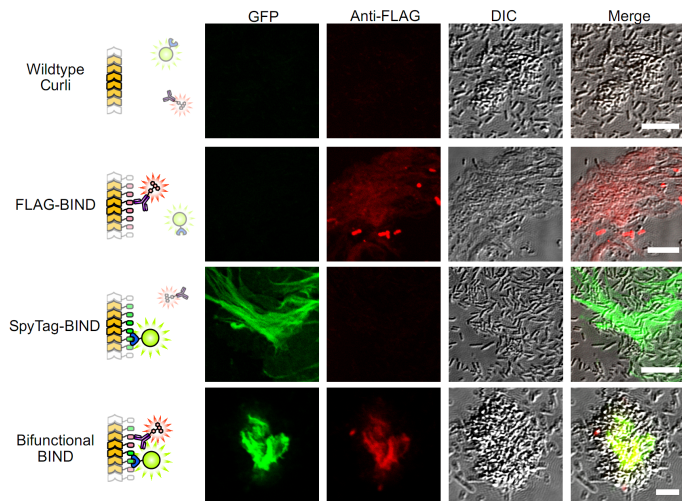


Figure 6.

1 **Discussion**

2 Here we have demonstrated a strategy, BIND, for the rational molecular design of a
3 microbial extracellular matrix component with the purpose of introducing new function into a
4 biofilm. The biofilms of *E. coli* are partly composed of a functional amyloid nanofiber, curli,
5 which plays a role in bacterial adhesion⁴⁴, aggregation⁴³, and biofilm stability^{37,45}. Our results
6 show that the curli system in *E. coli* is capable of secreting a wide variety of chimeric CsgA-
7 peptide constructs that can self-assemble into the extracellular matrix as amyloid nanofibers. The
8 fused peptide domains are displayed in high density on the network surface and maintain their
9 function even after assembly. The resulting nanofiber networks maintain their ability to
10 encapsulate the cells and show morphological heterogeneity, with some variants exhibiting the
11 tendency to form dense three-dimensional crypt-like structures or expansive fabric-like sheets
12 (Supplementary Figure 11). Indeed, further exploration of the ability to control the three-
13 dimensional morphology of curli-based nanostructures solely by altering the sequence of CsgA-
14 peptide fusions seems warranted. We then selected three of these artificially designed biofilm
15 materials to demonstrate that three distinct and diverse non-natural functions (silver nanoparticle
16 templating, strong adhesion to steel surfaces, and covalent protein immobilization) can be
17 introduced modularly into *E. coli* biofilms based on the predetermined functions of various
18 engineered peptide sequences. Our results show that biotemplating, substrate adhesion, and
19 protein immobilization can be readily programmed into a bacterial extracellular matrix.
20 Importantly, this was accomplished without the need for system re-optimization, suggesting that
21 other sequences can easily be incorporated into our system to access materials with a vast range
22 of non-natural functions. In addition, a co-culture of cells harboring different CsgA fusions

1 resulted in a bifunctional biofilm, suggesting that the modular aspect of our platform can be used
2 to engineer biofilms with a wide combination of desired functions.

3 The BIND technology lends itself to the rapid development of interfacial nanomaterials
4 with functions that can be drawn from the diverse repertoire of known natural and artificial
5 peptides and proteins. These biofilm-based materials can be used in a wide range of
6 environments that may or may not be conducive to cellular survival. In hospitable environments,
7 the encapsulated cells of the biofilm may be induced to self-regenerate or heal the material over
8 time, or remodel the material in response to environmental cues. In harsher environments, the
9 highly robust amyloid matrix, once assembled, could persist beyond the lifetime of the cellular
10 components as an acellular structure without the need for maintenance. In principle, our
11 approach can be used to introduce new function to many other microbial biofilms with analogous
12 functional amyloids (e.g., *Salmonella*⁴⁶, *Pseudomonas*⁴⁷, *Bacillus*⁴⁸ spp.) to capitalize on the
13 particular features of each wild-type strain. Given that the engineered bacteria proliferate rapidly
14 and require no petroleum-derived raw building blocks in order to biosynthesize the external
15 matrix, BIND may be useful as a scalable and green approach to fabricating customized
16 interfacial materials across a wide range of size scales and environments.

17 Recent work with synthetic gene circuits allows for the control of biofilm formation
18 and dispersal dynamics through the engineering of global biofilm regulatory proteins^{7,49,50}. Other
19 work has paved the way for the patterning and control of curli composition¹⁴. By combining such
20 biofilm control strategies with the ability to widely program the functional properties of the
21 extracellular matrix as we present here with BIND platform, we envision a merging of synthetic
22 biology and materials science approaches. This would allow the development of large-scale
23 programmable ‘living’ materials in which bacteria act as autonomous and self-replicating

1 distributed molecular factories for the production of large-scale materials. Additionally,
2 engineered complex genetic logic gates could be used to switch on one or more defined BIND
3 biofilms under specific environmental cues. This would potentially allow a single cell to encode
4 for tens and possibly hundreds of different artificial BIND variants that could dynamically alter
5 the bacterial ECM properties on demand.

6

7 **Methods**

8 **Cell strains and plasmids.** All cloning and protein production was performed in Mach1 (Life
9 Technologies, CA, USA) and Rosetta cells (EMD Millipore, CA, USA), respectively. The *csgA*
10 gene was isolated from *E. coli* K-12 genomic DNA and cloned into pBbE1a⁵¹, a ColE1 plasmid
11 under control of the Trc promoter (Addgene, MA, USA). Peptide insert regions were either fully
12 synthesized (Integrated DNA Technologies, IA, USA) or PCR-generated by overlap extension⁵².
13 All cloning was performed using isothermal Gibson Assembly⁵³ and verified by DNA
14 sequencing. The *csgA* deletion mutant LSR10 (MC4100, $\Delta csgA$) was a kind gift from the
15 Chapman Laboratory. The *csgA* deletion mutant PHL628- $\Delta csgA$ (MG1655, *malA-Kan* *ompR234*
16 $\Delta csgA$) was provided by the Hay Laboratory. All cell strains, plasmids, and primers used in this
17 study are fully provided in the supplementary section (Supplementary Tables 1, 2, and 3).

18 **Curli biofilm formation.** To produce curli, LSR10 cells or PHL628 cells were transformed with
19 pBbE1a plasmids encoding for CsgA or CsgA-peptide fusions. As a negative control, cells were
20 transformed with empty pBbE1a plasmid. The cells were then streaked or spotted onto YESCA-
21 CR plates⁵⁴, containing 10 g/L of casamino acids, 1 g/L of yeast extract, and 20 g/L of agar.
22 These plates were supplemented with 100 µg/mL of ampicillin, 0.5 mM of IPTG, 25 µg/mL of
23 Congo Red and 5 µg/mL of Brilliant Blue G250. The plates were then incubated for 48 hours at

1 25°C and then imaged to determine the extent of Congo Red binding. For the spotted plates, the
2 transformants were grown in YESCA liquid media supplemented with 100 µg/mL of ampicillin
3 and 0.2 mM of IPTG for 48 hours at 25°C before spotting 20 µL onto YESCA-CR plates.

4 **Scanning electron microscopy.** Curliated wild-type or BIND cell samples were either directly
5 taken from induced YESCA cultures or scraped from YESCA-CR plates and resuspended in
6 millipore H₂O. For SEM analysis, samples were applied to Nuclepore filters (0.22 µm pore size;
7 GE Healthcare Bio-Sciences, PA, USA) under vacuum, washed with millipore H₂O and fixed
8 with 2% glutaraldehyde + 2% paraformaldehyde overnight at 4°C, followed by fixation in 1%
9 osmium tetroxide. The samples were then washed in millipore H₂O, dehydrated with an
10 increasing ethanol step gradient, followed by a hexamethyldisilazane step gradient before gold
11 sputtering and analysis on a Zeiss Supra55VP FE-SEM.

12

1 **References**

- 2 1. Flemming, H.C. & Wingender, J. The biofilm matrix. *Nat Rev Microbiol* **8**, 623-33 (2010).
- 3 2. Römling, U. & Balsalobre, C. Biofilm infections, their resilience to therapy and innovative treatment strategies. *J Intern Med* **272**, 541-61 (2012).
- 4 3. Logan, B.E. Exoelectrogenic bacteria that power microbial fuel cells. *Nat Rev Microbiol* **7**, 375-81 (2009).
- 5 4. Singh, R., Paul, D. & Jain, R.K. Biofilms: implications in bioremediation. *Trends Microbiol* **14**, 389-97 (2006).
- 6 5. Halan, B., Buehler, K. & Schmid, A. Biofilms as living catalysts in continuous chemical syntheses. *Trends Biotechnol* **30**, 453-65 (2012).
- 7 6. Tsoligkas, A.N. *et al.* Engineering biofilms for biocatalysis. *Chembiochem* **12**, 1391-5 (2011).
- 8 7. Hong, S.H. *et al.* Synthetic quorum-sensing circuit to control consortial biofilm formation and dispersal in a microfluidic device. *Nat Commun* **3**, 613 (2012).
- 9 8. Chapman, M.R. *et al.* Role of Escherichia coli curli operons in directing amyloid fiber formation. *Science* **295**, 851-5 (2002).
- 10 9. Hammar, M., Arnqvist, A., Bian, Z., Olsén, A. & Normark, S. Expression of two csg operons is required for production of fibronectin- and congo red-binding curli polymers in Escherichia coli K-12. *Mol Microbiol* **18**, 661-70 (1995).
- 11 10. Smith, J.F., Knowles, T.P., Dobson, C.M., Macphee, C.E. & Welland, M.E. Characterization of the nanoscale properties of individual amyloid fibrils. *Proc Natl Acad Sci U S A* **103**, 15806-11 (2006).
- 12 11. Larsen, P., Nielsen, J.L., Otzen, D. & Nielsen, P.H. Amyloid-like adhesins produced by floc-forming and filamentous bacteria in activated sludge. *Appl Environ Microbiol* **74**, 1517-26 (2008).
- 13 12. Sivanathan, V. & Hochschild, A. Generating extracellular amyloid aggregates using E. coli cells. *Genes Dev* **26**, 2659-67 (2012).
- 14 13. Van Gerven, N. *et al.* Secretion and functional display of fusion proteins through the curli biogenesis pathway. *Mol Microbiol* **91**, 1022-35 (2014).
- 15 14. Chen, A.Y. *et al.* Synthesis and patterning of tunable multiscale materials with engineered cells. *Nat Mater* **13**, 515-23 (2014).
- 16 15. Giltner, C.L. *et al.* The Pseudomonas aeruginosa type IV pilin receptor binding domain functions as an adhesin for both biotic and abiotic surfaces. *Mol Microbiol* **59**, 1083-96 (2006).
- 17 16. Marcus, A., Sadimin, E., Richardson, M., Goodell, L. & Fyfe, B. Fluorescence microscopy is superior to polarized microscopy for detecting amyloid deposits in Congo red-stained trephine bone marrow biopsy specimens. *Am J Clin Pathol* **138**, 590-3 (2012).
- 18 17. Casadaban, M.J. Transposition and fusion of the lac genes to selected promoters in Escherichia coli using bacteriophage lambda and Mu. *J Mol Biol* **104**, 541-55 (1976).
- 19 18. Zogaj, X., Nimtz, M., Rohde, M., Bokranz, W. & Römling, U. The multicellular morphotypes of Salmonella typhimurium and Escherichia coli produce cellulose as the second component of the extracellular matrix. *Mol Microbiol* **39**, 1452-63 (2001).
- 20 19. Liu, D. & Reeves, P.R. Escherichia coli K12 regains its O antigen. *Microbiology* **140** (Pt 1), 49-57 (1994).

- 1 20. Teather, R.M. & Wood, P.J. Use of Congo red-polysaccharide interactions in enumeration
2 and characterization of cellulolytic bacteria from the bovine rumen. *Appl Environ Microbiol*
3 **43**, 777-80 (1982).
- 4 21. Hochuli, E., Bannwarth, W., Dobeli, H., Gentz, R. & Stuber, D. Genetic approach to
5 facilitate purification of recombinant proteins with a novel metal chelate adsorbent. *Nat*
6 *Biotech* **6**, 1321-25 (1988).
- 7 22. Kim, S.N. *et al.* Preferential binding of peptides to graphene edges and planes. *J Am Chem*
8 *Soc* **133**, 14480-3 (2011).
- 9 23. Hopp, T.P. *et al.* A short polypeptide marker sequence useful for recombinant protein
10 identification and purification. *Nat Biotech* **6**, 1204-10 (1988).
- 11 24. Pender, M.J., Sowards, L.A., Hartgerink, J.D., Stone, M.O. & Naik, R.R. Peptide-mediated
12 formation of single-wall carbon nanotube composites. *Nano Lett* **6**, 40-4 (2006).
- 13 25. Naik, R.R., Stringer, S.J., Agarwal, G., Jones, S.E. & Stone, M.O. Biomimetic synthesis
14 and patterning of silver nanoparticles. *Nat Mater* **1**, 169-72 (2002).
- 15 26. Chung, W.J., Kwon, K.Y., Song, J. & Lee, S.W. Evolutionary screening of collagen-like
16 peptides that nucleate hydroxyapatite crystals. *Langmuir* **27**, 7620-8 (2011).
- 17 27. Oren, E.E. *et al.* A novel knowledge-based approach to design inorganic-binding peptides.
18 *Bioinformatics* **23**, 2816-22 (2007).
- 19 28. Zakeri, B. *et al.* Peptide tag forming a rapid covalent bond to a protein, through engineering
20 a bacterial adhesin. *Proc Natl Acad Sci U S A* **109**, E690-7 (2012).
- 21 29. Zhou, W., Schwartz, D.T. & Baneyx, F. Single-pot biofabrication of zinc sulfide immuno-
22 quantum dots. *J Am Chem Soc* **132**, 4731-8 (2010).
- 23 30. Houston, M.E. *et al.* Binding of an oligopeptide to a specific plane of ice. *J Biol Chem* **273**,
24 11714-8 (1998).
- 25 31. Arakaki, A., Webb, J. & Matsunaga, T. A novel protein tightly bound to bacterial magnetic
26 particles in Magnetospirillum magneticum strain AMB-1. *J Biol Chem* **278**, 8745-50
27 (2003).
- 28 32. Taylor, J.D. *et al.* Atomic resolution insights into curli fiber biogenesis. *Structure* **19**, 1307-
29 16 (2011).
- 30 33. Sabaté, R. & Ventura, S. Cross- β -sheet supersecondary structure in amyloid folds:
31 techniques for detection and characterization. *Methods Mol Biol* **932**, 237-57 (2013).
- 32 34. Schütz, A.K. *et al.* The amyloid-Congo red interface at atomic resolution. *Angew Chem Int*
33 *Ed Engl* **50**, 5956-60 (2011).
- 34 35. Sivanathan, V. & Hochschild, A. A bacterial export system for generating extracellular
35 amyloid aggregates. *Nat Protoc* **8**, 1381-90 (2013).
- 36 36. Gebbink, M.F., Claessen, D., Bouma, B., Dijkhuizen, L. & Wösten, H.A. Amyloids--a
37 functional coat for microorganisms. *Nat Rev Microbiol* **3**, 333-41 (2005).
- 38 37. Hidalgo, G., Chen, X., Hay, A.G. & Lion, L.W. Curli produced by Escherichia coli
39 PHL628 provide protection from Hg(II). *Appl Environ Microbiol* **76**, 6939-41 (2010).
- 40 38. Vidal, O. *et al.* Isolation of an Escherichia coli K-12 mutant strain able to form biofilms on
41 inert surfaces: involvement of a new ompR allele that increases curli expression. *J Bacteriol*
42 **180**, 2442-9 (1998).
- 43 39. Reguera, G. *et al.* Extracellular electron transfer via microbial nanowires. *Nature* **435**,
44 1098-101 (2005).
- 45 40. Hochbaum, A.I. & Aizenberg, J. Bacteria pattern spontaneously on periodic nanostructure
46 arrays. *Nano Lett* **10**, 3717-21 (2010).

- 1 41. Lewandowski, Z., Beyenal, H., Myers, J. & Stookey, D. The effect of detachment on
2 biofilm structure and activity: the oscillating pattern of biofilm accumulation. *Water Sci*
3 *Technol* **55**, 429-36 (2007).
- 4 42. Horn, H., Reiff, H. & Morgenroth, E. Simulation of growth and detachment in biofilm
5 systems under defined hydrodynamic conditions. *Biotechnol Bioeng* **81**, 607-17 (2003).
- 6 43. Zhou, Y. *et al.* Promiscuous cross-seeding between bacterial amyloids promotes
7 interspecies biofilms. *J Biol Chem* **287**, 35092-103 (2012).
- 8 44. Pawar, D.M., Rossman, M.L. & Chen, J. Role of curli fimbriae in mediating the cells of
9 enterohaemorrhagic Escherichia coli to attach to abiotic surfaces. *J Appl Microbiol* **99**, 418-
10 25 (2005).
- 11 45. Kikuchi, T., Mizunoe, Y., Takade, A., Naito, S. & Yoshida, S. Curli fibers are required for
12 development of biofilm architecture in Escherichia coli K-12 and enhance bacterial
13 adherence to human uroepithelial cells. *Microbiol Immunol* **49**, 875-84 (2005).
- 14 46. White, A.P. *et al.* High efficiency gene replacement in Salmonella enteritidis: chimeric
15 fimbriins containing a T-cell epitope from Leishmania major. *Vaccine* **17**, 2150-61 (1999).
- 16 47. Dueholm, M.S. *et al.* Functional amyloid in Pseudomonas. *Mol Microbiol* **77**, 1009-20
17 (2010).
- 18 48. Romero, D., Aguilar, C., Losick, R. & Kolter, R. Amyloid fibers provide structural integrity
19 to Bacillus subtilis biofilms. *Proc Natl Acad Sci U S A* **107**, 2230-4 (2010).
- 20 49. Ma, Q., Yang, Z., Pu, M., Peti, W. & Wood, T.K. Engineering a novel c-di-GMP-binding
21 protein for biofilm dispersal. *Environ Microbiol* **13**, 631-42 (2011).
- 22 50. Hong, S.H., Lee, J. & Wood, T.K. Engineering global regulator Hha of Escherichia coli to
23 control biofilm dispersal. *Microb Biotechnol* **3**, 717-28 (2010).
- 24 51. Lee, T.S. *et al.* BglBrick vectors and datasheets: A synthetic biology platform for gene
25 expression. *J Biol Eng* **5**, 12 (2011).
- 26 52. Horton, R.M., Hunt, H.D., Ho, S.N., Pullen, J.K. & Pease, L.R. Engineering hybrid genes
27 without the use of restriction enzymes: gene splicing by overlap extension. *Gene* **77**, 61-8
28 (1989).
- 29 53. Gibson, D.G. *et al.* Enzymatic assembly of DNA molecules up to several hundred
30 kilobases. *Nat Methods* **6**, 343-5 (2009).
- 31 54. Benhold, H. Specific staining of amyloid by Congo red. *Muenchen Med Wochenschr*,
32 1537-38 (1922).
- 33

34 **Acknowledgements**

35 This work was funded by the Wyss Institute for Biologically Inspired Engineering. Z.B.
36 acknowledges the NSF GRF for funding. P.R.T. is grateful for funding from the A*STAR
37 National Science Graduate Fellowship (Singapore). The authors thank Professor Matthew R.
38 Chapman (University of Michigan) for the kind donation of the LSR10 *E. coli* strain, the anti-
39 CsgA antibody, and assistance with technical queries. The authors also thank Professor Anthony

1 G. Hay (Cornell University) for providing the PHL628- Δ csgA strain. The AgfA homology model
2 protein structure was graciously provided by Professor Aaron P. White (University of
3 Saskatchewan).

4 **Author Contributions**

5 P.Q.N and N.S.J. conceived of the concept, designed the research, and analyzed the data.
6 P.Q.N., Z.B., and P.R.T. performed research and analyzed the data. P.Q.N. and N.S.J. wrote the
7 paper with discussions and contributions from all other authors. All authors discussed the results
8 and commented on the manuscript.

9 **Competing Financial Interests**

10 The authors have applied for a patent based on this work

11

12 **Figure Legends**

13 **Figure 1 | Genetic programming and modularity of the BIND system.** In the BIND platform,
14 Δ csgA cells heterologously express and secrete fusion proteins consisting of an amyloidogenic
15 domain (CsgA, shown in orange) and a functional peptide domain (green). This secreted fusion
16 protein self-assembles into an extracellular network of amyloid nanofibers that are anchored
17 onto the cell surface, resulting in a biofilm material with programmed non-natural functions. A
18 three-dimensional protein model is shown of the self-assembling and functional peptide
19 domains, using homology model protein threading of the CsgA sequence onto an AgfA
20 structure. An example peptide domain, SpyTag (see Table 1), is shown in green and the 6-
21 residue flexible linker in gray. The peptide structure was predicted using PepFold and all
22 structural manipulation performed in PyMol.

23 **Figure 2 | Genetic engineering of the BIND platform.** (a) A library of CsgA fusion mutants in
24 which the MBD peptide insert (purple) was placed at the N- or C-terminus of the curlin repeat
25 domains (red) and flanked by a 6-residue linker, 2-residue linker, or no linker (green). (b) The
26 MBD insert library was transformed into LSR10 (MC4100, Δ csgA) cells and streaked onto
27 YESCA-Congo Red induction plates. Red staining indicates amyloid production. (c) A
28 representative set of culture spots of a BIND library consisting of 12 various functional peptides
29 on YESCA-Congo Red induction plates (enumerated in Table 1). (d) Quantitative Congo Red
30 values were obtained from quadruplicate YESCA-CR spotted cultures using intensity
31 quantitation (ImageJ) measurements of the relative amyloid produced for each CsgA-peptide
32 fusion, normalized to wild-type CsgA. Standard error is shown. (e) Whole-cell filtration ELISA
33 using an anti-CsgA antibody (black bars); secondary antibody-only controls are shown as grey
34 bars. Each experiment was performed in triplicate and standard error is shown. FE-SEM images
35 of the peptide fusion BIND library transformed into LSR10 (MC4100, Δ csgA) cells with no CsgA

1 (f), wild-type CsgA (g), and the BIND peptide panel (see Table 1): HIS (h), GBP (i), FLAG (j),
2 CNBP (k), A3 (l), CLP12 (m), QBP1 (n), SpyTag (o), MBD (p), CT43 (q), AFP8 (r), and Mms6
3 (s). All scale bars are 1 μ m.

4 **Figure 3 | Nanoparticle templating by BIND.** Silver nanoparticles were templated by A3-BIND
5 biofilms incubated in aqueous AgNO₃. Representative TEM micrographs demonstrate that
6 PHL628 Δ csgA cells producing wild-type CsgA (a) show no nanoparticle templating, whereas
7 A3-BIND (b) templates nanoparticles after incubation in 147mM AgNO₃ for 4 hours. (c) A higher
8 magnification of the Ag nanoparticles organized on A3-BIND nanofilaments is shown. All scale
9 bars are 0.5 μ m.

10 **Figure 4 | BIND biofilms can be programmed to adhere to specific substrates.** (a)
11 Adhesion of PHL628 Δ csgA cells producing no CsgA (left), wild-type CsgA (middle), and CsgA-
12 MBD (right) was tested by spotting induced cultures onto a 304L steel coupon and incubating
13 for 48 hours at 4°C. The ring formation is due to cells being drawn to the edges of the droplet
14 during drying, known as the “coffee ring effect”. (b)The MBD-BIND biofilms were analyzed by
15 FE-SEM. Scale bar is 250 μ m. (c) magnification of the boxed area in (b) of a false-colored FE-
16 SEM micrograph showing MBD-BIND cells adhered to the 304L surface. Scale bar is 10 μ m. (d)
17 magnification of the boxed area in (c) of a false-colored FE-SEM micrograph showing a
18 zoomed-in view of the cell bodies. Due to the vigorous washing process, some of the cell bodies
19 appear damaged. Scale bar is 2 μ m.

20 **Figure 5 | Covalent immobilization of full-length proteins onto SpyTag-BIND biofilms.** (a)
21 The BIND immobilization strategy which uses an isopeptide bond forming split-protein S.
22 *pyogenes* FbaB adhesin system²⁸ to covalently attach proteins fused to the SpyCatcher domain
23 onto BIND biofilms displaying the 13-residue SpyTag. TEM and FE-SEM images, respectively,
24 of PHL628 Δ csgA strains expressing no curli (b, e), wild-type CsgA (c, f), and the SpyTag-BIND
25 biofilms (d, g); scale bars are 1 μ m. (h) SpyTag-BIND biofilms were grown on PLL-modified
26 glass substrates and then visualized with a nucleic-acid stain (SYTO61) followed by incubation
27 with a cell lysate containing GFP-SpyCatcher fusion protein; scale bars are 25 μ m.
28 Epifluorescence microscopy of the biofilms reveals that only the proper combination of CsgA-
29 SpyTag-BIND biofilms and GFP-SpyCatcher protein-containing cell lysate results in significant
30 protein immobilization (top row). In contrast, SpyTag-BIND biofilms combined with a GFP-
31 SpyCatcher_{E77Q} protein that has a key catalytic residue mutated in the SpyCatcher domain
32 showed no immobilization (middle row). Wild-type CsgA biofilms combined with GFP-
33 SpyCatcher also do now show significant immobilization.

34
35 **Figure 6 | BIND can be used to generate programmable multifunctional biofilms.** Wild-type
36 CsgA, FLAG-BIND, SpyTag-BIND, and a co-culture of FLAG-BIND and SpyTag-BIND were all
37 probed with GFP-SpyCatcher followed by anti-FLAG DyLight650 conjugated antibody. Confocal
38 microscopy images for the GFP, DyLight650, and DIC channels are shown. All scale bars are 5
39 μ m.

40

41

42

43

1 Tables.

Table 1 | Functional Peptide Library Incorporated into BIND

Peptide	Sequence	Length (aa)	Type	Specific Function	Reference
HIS	HHHHHH	6	Affinity Tag	Affinity Tag	21
GBP	EPLQLKM	7	Substrate Binding	Graphene edge binding	22
FLAG	DYKDDDDK	8	Affinity Tag	Affinity Tag	23
CNBP	HSSYWYAFNNKT	12	Substrate Binding	Carbon nanotube binding	24
A3	AYSSGAPPMPFF	12	Substrate Binding	Gold surface binding	25
CLP12	NPYHPTIPQSVH	12	Mineral templating	Hydroxyapatite nucleation	26
QBP1	PPPWLPMPPWS	12	Substrate Binding	Quartz/Glass binding	27
SpyTag	AHIVMVDAYKPTK	13	Protein Display	Covalent capture/display of proteins	28
CT43	CGPAGDSSGVDSRSGPC	18	NP templating	ZnS templating	29
MBD	KCTSDQDEQFIPKGCSKGSGGSG	23	Substrate Binding	Binding to stainless steel surfaces	15
AFP8	DTASDAAAAAALTAAANAKAAAELTAANAAAAAAATAR	37	Substrate Binding	Ice crystal binding	30
Mms6	GGTIWTGKGLGLGLGAWGPILGVVGAGAVYAYMKSRDIESAQSDDEEVELRDALA	59	NP templating	Magnetite templating	31

2